Tidal Bore Research: Field Works, Physical Modeling, CFD & More

Hubert Chanson
Professor, The University of Queensland, School of Civil Engineering, Brisbane QLD4072, Australia.
E-mail: h.chanson@uq.edu.au

ABSTRACT: A tidal bore is a series of waves propagating upstream as the tidal flow turns to rising in a river mouth during the early flood tide. The application of continuity and momentum principles gives a complete solution of the ratio of the conjugate cross-section areas as a function of the upstream Froude number $Fr_1 = (U+V_1)/(g \times A_1/B_1)_{1/2}$. Theoretical considerations are developed in terms of the effects of flow resistance and bed slope. Physically the tidal bore propagation induces a massive mixing of the natural system. Prototype observations highlighted that the tidal bore passage is associated with large fluctuations in water depth and instantaneous velocity components. Both experimental and numerical studies indicated the production of large coherent structures advected behind the tidal bore. The presence of such large-scale coherent structures indicated that a great amount of sediment materials could be placed into suspension and transported by the flood tide flow in a natural system. Future research into tidal bores should combine computational calculations combined with ad-hoc laboratory measurements, and it must be complemented by detailed field measurements in natural systems.

KEY WORDS: Tidal bores, Theoretical analysis, Physical modelling, Laboratory experiments, Field measurements, Computational fluid dynamics, Numerical modeling, Environmental impact.

1 INTRODUCTION

A tidal bore is a series of waves propagating upstream in an estuarine zone, as the tidal flow turns to rising. It is a rapidly-varied unsteady open channel flow generated by the relatively rapid rise in water elevation at the river mouth during the early flood tide, when the tidal range exceeds 4.5 to 6 m and the funnel shape of both river mouth and lower estuarine zone amplifies the tidal wave. The driving process is the large tidal amplitude and its amplification in the estuarine system (Tricket 1965). After formation, the bore is characterised by an abrupt rise in water surface elevation at the bore leading edge, which is a singularity in terms of pressure and velocity fields. Figure 1 illustrates some tidal bores in China, Mexico and France. Pertinent accounts include Moore (1888), Moule (1923) and Chanson (2011a). The existence of the tidal bore is based upon a delicate balance between the tidal amplitude, the freshwater river flow conditions and the estuarine channel bathymetry. This balance may be easily disturbed by changes in boundary conditions and freshwater runoff (Chanson 2011a). A number of man-made interventions led to the modification and sometimes disappearance of tidal bores in France, Canada, Mexico for example. While the fluvial navigation gained in safety, the ecology of the estuarine systems was affected adversely, e.g. with the disappearance of native fish species. Some natural events may also affect the tidal bores: e.g., the 1964 Alaska earthquake on the Turnagain and Knik Arms bores, the combination of storm surge and spring tide in Bangladesh in November 1970, the 2001 flood of the Ord River (Australia), the 2010 El Mayor-Cucapah earthquake on the Colorado River bore.

A related process is the tsunami-induced bore. When a tsunami wave propagates upriver, its leading

edge is led by a positive surge. The tsunami-induced bore may propagate into the riverine system far upstream, as observed in Japan in 1983, 2001, 2003 and 2011 (Tanaka et al. 2012), during the 26 December 2004 tsunami disaster in the Indian Ocean, and in the River Yealm in United Kingdom on 27 June 2011.

In this contribution, the author reviews the basic theoretical developments, before discussing the physical modelling of tidal bores. A number of recent field measurements are presented and the results are compared with a series of laboratory experiments. Recent progresses in computational fluid dynamics (CFD) modelling are discussed. Lastly the progresses for the last twenty years are critically considered before future research directions are outlined.

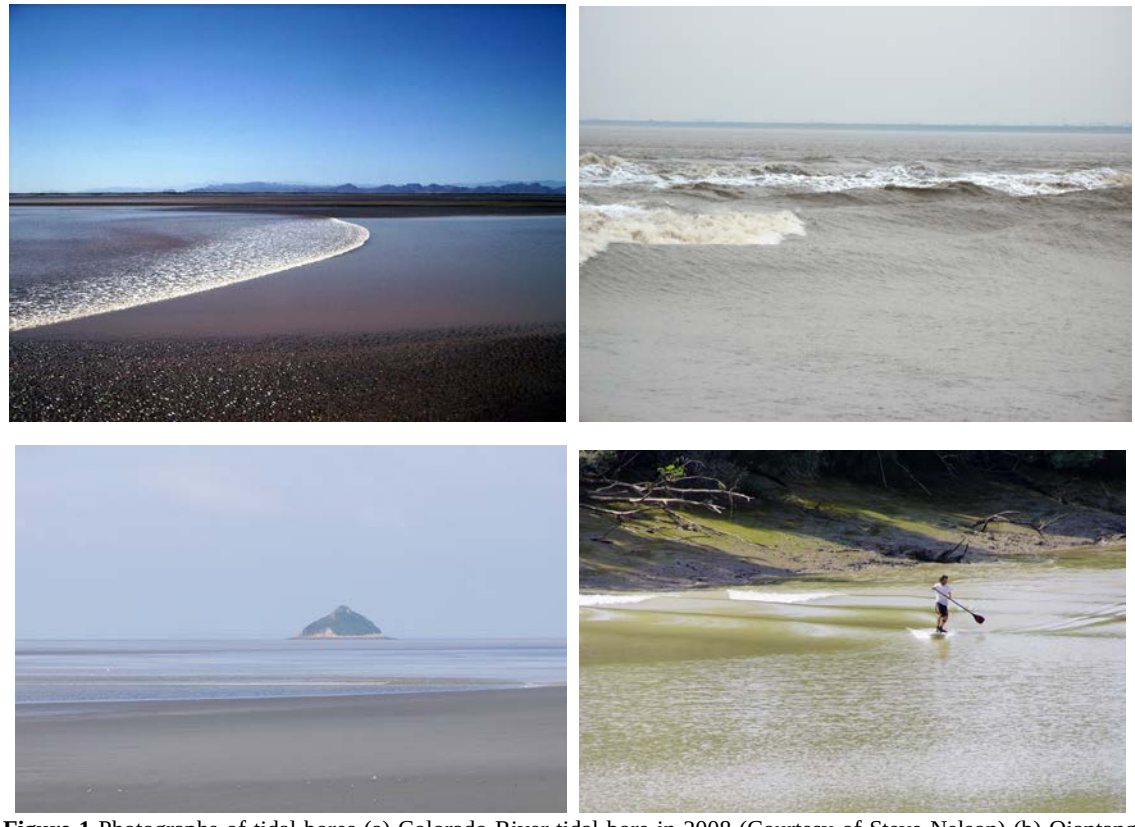

Figure 1 Photographs of tidal bores (a) Colorado River tidal bore in 2008 (Courtesy of Steve Nelson) (b) Qiantang River bore on 23 July 2009 (Courtesy of Jean-Pierre and Claudine Girardot) (c) Sélune River bore on 23 June 2012 (d) Surfer on the Garonne River bore at Arcins on 3 July 2012

2 THEORY

2.1 Momentum integral equation

The driving process of the tidal bore phenomenon is a large tidal range which may be locally amplified by a number of factors: for example, when the natural resonance period of the estuary is close to the tidal period. When the sea level rises with time during the early flood tide, the tidal wave steepness increases with distance from the river mouth until the leading edge of the tidal wave becomes an abrupt front: that is, the tidal bore. The inception and development of a tidal bore may be predicted using the shallow-water equations (e.g. Saint-Venant equations) and the method of characteristics. After formation, the tidal bore is characterised by an abrupt rise in water depth (Fig. 1), and the bore front may be analysed as a hydraulic jump in translation (Lighthill 1978, Liggett 1994).

In the system of reference in translation with the bore, the integral form of the continuity and momentum equations gives:

$$(V_1 + U) \times A_1 = (V_2 + U) \times A_2 \quad (1)$$

$$\rho \times (V_1 + U) \times A_1 \times (\beta_1 \times (V_1 + U) - \beta_2 \times (V_2 + U)) = \iint_{A_2} P \times dA - \iint_{A_1} P \times dA + F_{fric} - W \times \sin\theta \quad (2)$$

in which V is the flow velocity positive downstream, U the bore celerity positive upstream, ρ is the water density, g the gravity acceleration, A the channel cross-sectional area measured perpendicular to the flow direction, β a momentum correction coefficient, P the pressure, F_{fric} the flow resistance force, W the weight force, θ the angle between the bed slope and horizontal, and the subscripts 1 and 2 refer to the initial flow conditions and the flow conditions immediately after the tidal bore respectively (Fig. 2).

Neglecting the flow resistance, the effect of the velocity distribution ($\beta_1 = \beta_2 = 1$) and for a flat horizontal channel ($\sin\theta \approx 0$), Equations (1) and (2) give a relationship between the ratio of conjugate cross-section areas A_2/A_1 and tidal bore Froude number (Chanson 2012):

$$\frac{A_2}{A_1} = \frac{1}{2} \times \frac{\sqrt{\left(2 - \frac{B'}{B}\right)^2 + 8 \times \frac{\frac{B'}{B}}{\frac{B_1}{B}} \times Fr_1^{\,2}} - \left(2 - \frac{B'}{B}\right)}{\frac{B'}{B}} \quad (3)$$

where Fr_1 is the Froude number is defined as:

$$Fr_1 = \frac{U + V_1}{\sqrt{g \times \frac{A_1}{B_1}}} \quad (4)$$

B' is a characteristic cross-sectional width fulfilling:

$$\int_{A_1}^{A_2} \rho \times g \times (d_2 - y) \times dA = \frac{1}{2} \times \rho \times g \times (d_2 - d_1)^2 \times B' \quad (5)$$

d is the water depth, and B is another characteristic width such as:

$$B = \frac{A_2 - A_1}{d_2 - d_1} \quad (6)$$

Equation (3) yields an analytical solution of the ratio of cross-sectional areas as a function of the Froude number and dimensionless characteristic widths B'/B_1 and B/B_1. The effects of the celerity are linked implicitly with the initial flow conditions, including for a fluid initially at rest ($V_1 = 0$) and for a stationary jump ($U = 0$). Several prototype observations of tidal bores were documented with detailed hydrodynamic and bathymetric conditions, and the data are summarised in Figure 3. Figure 3a (Left) shows the relationship between the characteristic widths B, B' and B_2 and the Froude number. Figure 3b (Right) presents the ratio of conjugate cross-section areas as a function of the Froude number, and the data are compared with Equation (3) for irregular channel cross-sections and with the Bélanger equation for a prismatic rectangular channel. The results highlighted the effects of the irregular cross-sectional shape. For example, the Bélanger equation was unsuitable for a tidal bore in an irregular channel. Morever the traditional approximation $Fr_1 = V_1/(g \times d_1)^{0.5}$ would yield errors between 12% and 74% for the data listed in Figure 3.

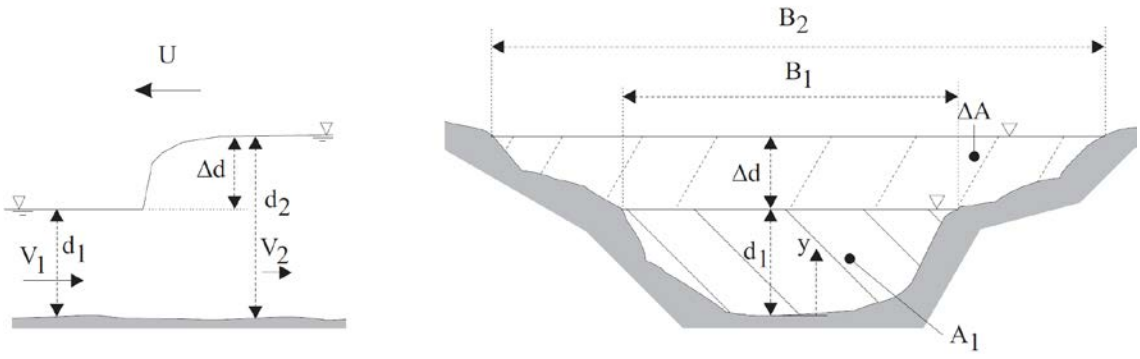

Figure 2 Definition sketch of a tidal bore propagating upstream

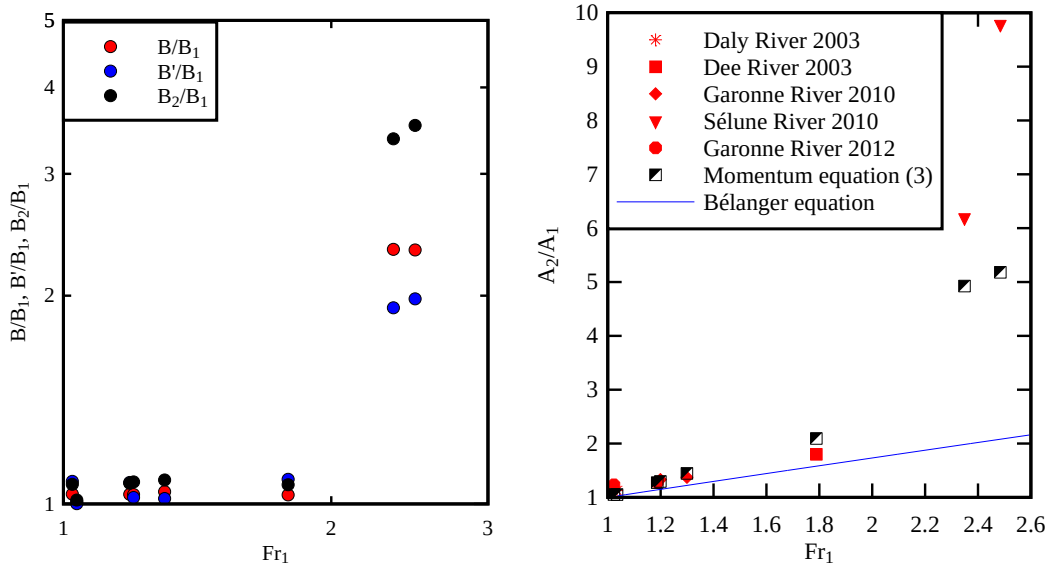

Figure 3 Application of the momentum principle to tidal bores in irregular cross-section channels (Simpson et al. 2004, Wolanski et al. 2004, Mouazé et al. 2010, Chanson et al. 2011, Reungoat et al. 2012) - (a, Left) Characteristic free-surface width (field data); (b, Right) Comparison between Equation (3), Bélanger equation and field data

2.2 Case studies

In presence of boundary friction and bed form drag losses, the flow resistance force F_{fric} is non-zero and the equation of conservation of momentum (Eq. (2)) may be solved analytically for a flat horizontal channel. The combination of the equations of conservation of mass and momentum gives:

$$Fr_1 = \sqrt{\frac{1}{2} \times \frac{A_2}{A_1} \times \frac{B_1}{B} \times \left(\left(2 - \frac{B'}{B} \right) + \frac{B'}{B} \times \frac{A_2}{A_1} \right) + \frac{A_2}{A_2 - A_1} \times \frac{F_{fric}}{\rho \times g \times \frac{{A_1}^2}{B}}} \quad (7)$$

Equation (7) accounts for the effects of bed friction on the tidal bore properties in a irregular channel. The theoretical result implies a smaller ratio of the conjugate depths d_2/d_1 with increasing flow resistance (Chanson 2012). The finding shows further that the effects of flow resistance decrease with increasing Froude number and become negligible for Froude numbers greater than 2 to 3 depending upon the cross-sectional properties.

Considering a tidal bore propagating upstream in a smooth sloping rectangular prismatic channel, the combination of the continuity and momentum principles gives a physically meaningful solution

assuming $\cos\theta \approx 1$, where θ is the angle between the bed slope and horizontal, positive for a channel sloping downwards in the downstream direction. Namely the ratio of conjugate depths equals:

$$\frac{d_2}{d_1} = \frac{1}{2} \times \left(\sqrt{(1-\varepsilon)^2 + 8 \times \frac{Fr_1^2}{1-\varepsilon}} - (1-\varepsilon) \right) \quad (8)$$

where d_1 and d_2 are initial and new flow depths respectively, and ε is a dimensionless coefficient defined as

$$\varepsilon = \frac{Vol \times \sin\theta}{B_1 \times d_1^2 \times (Fr_1^2 - 1)} \quad (9)$$

with B_1 the channel width and Vol the volume of the control volume encompassing the bore front, such as $W = \rho \times g \times Vol$. Equation (9) implies that the ratio of conjugate depths increases with increasing bed slope for a given Froude number.

For a smooth horizontal rectangular prismatic channel, Equations (3), (7) and (8) yield to the Bélanger equation:

$$\frac{d_2}{d_1} = \frac{1}{2} \times \left(\sqrt{1 + 8 \times Fr_1^2} - 1 \right) \quad (10)$$

2.3 Similitude and modelling

In any study of tidal bores, the relevant parameters required for a dimensional analysis encompass the fluid properties and physical constants, the channel geometry and initial conditions, and the tide properties. Considering a tidal bore propagating in a fixed boundary channel, a simplified dimensional analysis yields:

$$\frac{P}{\rho \times g \times d_1}, \frac{V_x}{V_1}, \frac{V_y}{V_1}, \frac{V_z}{V_1} = F\left(\frac{x}{\frac{A_1}{B_1}}, \frac{y}{\frac{A_1}{B_1}}, \frac{z}{\frac{A_1}{B_1}}, t \times \sqrt{\frac{g}{A_1 / B_1}}, Fr_1, Re_1, Mo, \frac{A_1}{B_1 \times d_1}, \frac{B}{B_1}, \frac{B'}{B_1}, \theta, k_s, ... \right) \quad (11)$$

where P is the instantaneous pressure, V_x, V_y, V_z are the longitudinal, transverse and vertical velocity components respectively at a location (x, y, z) and time t, x is the coordinate in the flow direction, y is the horizontal transverse coordinate measured from the channel centreline, z is the vertical coordinate measured from channel bed, t is the time, Re_1 is the Reynolds number: $Re_1 = \rho \times (V_1+U) \times A_1/(\mu \times B_1)$, Mo is the Morton number: $Mo = g \times \mu^4/(\rho \times \sigma^3)$, ρ and μ are the water density and dynamic viscosity respectively, σ is the surface tension between air and water, and k_s is an equivalent sand roughness height. Equation (11) expresses the dimensionless relationships between the turbulent flow properties at a position (x,y,z) at a time t and the tidal bore properties, initial flow properties, channel geometry and fluid properties. The tidal properties are implicitly incorporated in the form of the bore celerity in the Froude and Reynolds number definitions. Note that the biochemical properties of the water solution may be considered especially in natural estuarine systems, while the compressibility of entrained air bubbles might be relevant in breaking bores. Further the sediment properties should be considered in a natural system with movable boundaries.

In a geometrically similar model, the flow must be dynamically similar to that in the prototype. A true dynamic similarity is achieved only if each dimensionless term has the same value in model and prototype. Scale effects might exist when one or more Π-terms have different values between model and prototype. In tidal bore and hydraulic jump studies, a Froude similitude is selected because of theoretical considerations (Eq. (3)) (Docherty and Chanson 2012). Viscous scale effects may occur unless the Reynolds number is large enough for the viscous terms to be small compared with other terms in the basic equations.

3 FIELD MEASUREMENTS

For a tidal bore, theoretical considerations demonstrate that a key dimensionless parameter is the Froude number (Eq. (4)) which characterises the strength of the bore. When the Froude number Fr_1 is less than one, the bore cannot form. For a Froude number between 1 and 1.4 to 1.8, the bore has an undular form: that is, the front is a smooth wave followed by a train of quasi-periodic secondary waves called whelps or undulations. An undular non-breaking bore is illustrated in Figure 1d. In an undular bore, the rate of energy dissipation is small to negligible, and the pressure distributions are not hydrostatic (Lemoine 1948, Chanson 2010a). Field and laboratory data showed a maximum in dimensionless wave amplitude and steepness for Fr_1 = 1.3 to 1.4, corresponding to the apparition of some slight breaking at the first wave crest. For larger Froude numbers (Fr_1 > 1.4 to 1.8), the tidal bore has a breaking front with a marked roller. Examples are shown in Figures 1a and 1c. The roller toe is a flow singularity: both air entrapment and intense turbulent mixing are generated at the toe, with increasing mixing and air entrainment in the roller with increasing Froude number. Both the roller height and size increase with increasing Froude number.

All field observations to date highlighted the intense turbulent mixing generated by the tidal bore (Fig. 1, Table 1). A related feature is the number of field work incidents, encompassing studies in the Dee River, Rio Mearim, Daly River, Garonne River and Sélune River (Kjerve and Ferreira 1993, Simpson et al. 2004, Wolanski et al. 2004, Mouazé et al. 2010, Reungoat et al. 2012). All the field studies stressed the power of the tidal bore motion and following flood tide.

Table 1 Detailed field measurements of tidal bores

River	Date	Bore type	Fr_1	d_1 (m)	Instrument
Dee (UK)	2/07/03	Breaking	1.04	1.50	ADCP
Daly (Australia)	6/09/03	Undular	1.79	0.72	ADVP
Garonne (France)	10/08/10	Undular	1.30	1.77	ADV
	11/09/10	Undular	1.20	1.81	ADV
Sélune (France)	24/09/10	Breaking	2.35	0.38	ADV
	25/09/10	Breaking	2.48	0.33	ADV
Garonne (France)	12/6/13	Undular	1.02	3.85	ADV
	12/6/13	Undular	1.19	4.58	ADV

References:
Simpson et al. (2004), Wolanski et al. (2004), Chanson et al. (2011), Mouazé et al. (2010), Reungoat et al. (2012)

The upstream propagation of a tidal bore is associated with a sudden rise in free-surface elevation: the passage of the bore creates a discontinuity in terms of the flow depth as well as a rapid variation of the velocity and pressure fields. The upstream advancement of the bore is followed by large, long-lasting fluctuations of the free-surface and instantaneous velocity and pressure. Some field observations are presented in Figure 4 for an undular bore (Fig. 4a) and a breaking bore (Fig. 4b). Figure 4 presents the dimensionless water depth as a function of a dimensionless time (t-T) where T is the time of passage of the bore front. All the prototype velocity data showed a rapid deceleration of the flow during the passage of the bore as illustrated in Figure 4. In Figure 4, the data are presented in a dimensionless form based upon the momentum considerations developed above. In most natural estuaries, the bore passage is associated with a flow reversal (V_x < 0) although not always (Bazin 1865, Kjerfve and Ferreira 1993, Reungoat et al. 2012). Some large fluctuations of all velocity components were observed during and after the bore at all vertical elevations within the water column. Both the visual observations and velocity measurements showed that the bore acted as a hydrodynamic shock associated with a sudden change in water depth and velocities. The bore was always followed by some relatively-long-period oscillations superposed to some high-frequency turbulent fluctuations with long lasting effects. The former may be linked with the formation, development and advection of large-scale coherent structures behind the front, as hinted by some recent numerical simulations (e.g. Lubin et al. 2010, Simon et al. 2011) and laboratory experiments (Chanson 2010b,2011b, Docherty and Chanson 2012). The turbulent velocity measurements indicated the existence of energetic turbulent events during and behind the tidal bore (Fig. 4). For

example, for $180 < (t-T)\times(g/(A_1/B_1))^{1/2} < 300$ in Figure 4a, and for $200 < (t-T)\times(g/(A_1/B_1))^{1/2} < 300$ and $350 < (t-T)\times(g/(A_1/B_1))^{1/2}$ in Figure 4b. These were highlighted by large and rapid f1uctuations of turbulent velocities and Reynolds stresses. The duration of the turbulent events appeared to be larger beneath undular bores, and shorter and more intense beneath breaking bores. Such macro-turbulence can maintain its coherence as the large-scale eddies are advected upstream behind the bore front. Importantly the macro-turbulence may contribute to significant sediment erosion from the bed and banks, and the upstream advection of the eroded material, as proposed by Chanson (2010b) and Docherty and Chanson (2012), together with the selective dispersion of neutrally-buoyant particles: e.g., fish eggs (Chanson and Tan 2010).

During the bore passage, the unsteady turbulent flow motion was characterised by large turbulent stresses, and turbulent stress fluctuations, beneath the front and during the whelp motion. The turbulent stress magnitudes were larger than in the initial turbulent flow shortly prior to the bore, thus highlighting the intense turbulent mixing beneath the tidal bore (Mouazé et al. 2010, Chanson et al. 2011). The field data showed that the instantaneous Reynolds stress magnitudes were larger than the critical threshold for sediment motion, although the comparison is restricted because the large scale vortices play an important role in terms of sediment material pickup and upward advection.

Overall the field data illustrated consistently that the tidal bore induced an intense mixing of the water column, for which the 'classical' mixing theories do not account. During the bore passage, the eroded bed material, scalars and particulates were advected upstream behind the tidal bore front. The results were consistent with the accretion and deposition of sediment materials in the upper estuarine zones of tidal-bore affected estuaries.

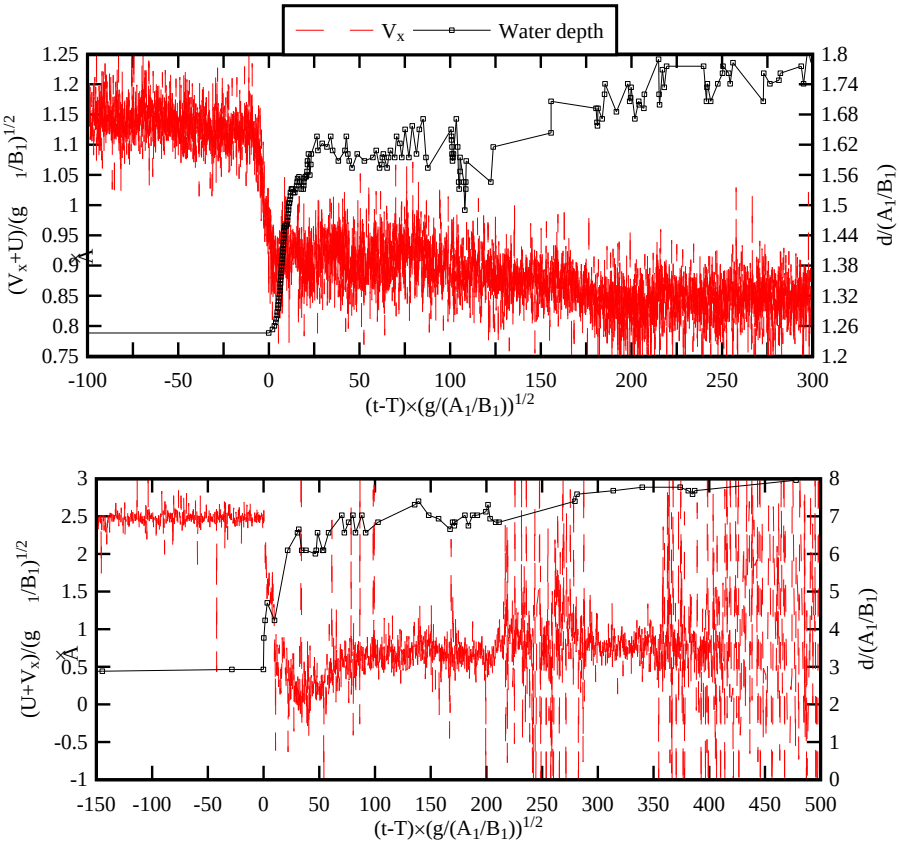

Figure 4 Dimensionless water depth and longitudinal velocity components during the passage of a tidal bore: prototype observations - (a, Top) Undular bore of the Garonne river on 11 September 2010, data collected 0.81 m beneath the free-surface (Data: Chanson et al. 2011); (b, Right) Breaking bore of the Sélune River on 25 September 2010, data collected at z = 0.10 m (Data: Mouazé et al. 2010)

4 NUMERICAL MODELLING

A number of numerical models were developed based upon the depth-averaged shallow-water equations. The results were generally in close agreement with the physical data, although the accuracy of natural system models was closely linked with some detailed bathymetric data and selection of friction coefficients (Benet and Cunge 1971, Madsen et al. 2005). For the Qiantang River bore, Madsen et al. (2005) achieved some successful comparison between field data and numerical modelling calculations in terms of free-surface elevations, only "*after an extensive calibration phase involving a sensitivity study of boundary conditions, bottom friction, and local bathymetric modifications*". In a simple rectangular channel, an one-dimensional model tended to overestimate the bore celerity and to underestimate its height close to the generation point (Reichstetter 2011). Importantly the depth-averaged models do not typically account for the intense mixing induced by the bore and their application can only be limited to simplistic case studies.

Some two-dimensional computational fluid dynamics (CFD) models were conducted with commercial softwares and university codes (Furuyama and Chanson 2010, Lubin et al. 2010, Reichstetter 2011). Although the results were qualitatively in agreement with laboratory visualisations, most numerical data could not match closely the experimental data without some gross approximations: e.g., in terms of the generation process, initial flow conditions, and boundary conditions. Most comparative data emphasised the complicated turbulent flow field and its unsteadiness under a tidal bore. In one case (at least), the comparison with laboratory data was poor: "*none of the Flow-3D^{TM} simulations provided good agreement with the physical data*" (Reichstetter 2011).

Some promising numerical data derived from a three-dimensional solution of the Navier-Stokes equations in air and water coupled with a subgrid scale turbulence model (large eddy simulation LES), the interface tracking being achieved by a volume of fluid (VOF) method (Simon et al. 2011, Chanson et al. 2012). A typical result is presented in Figure 5. Despite the extensive CPU requirements, the numerical data reproduced well the complicated three-dimensional interface deformations as illustrated in Figure 5. The preliminary results were encouraging and further developments are on-going.

The experience gained with CFD modelling highlighted the massive CPU requirements, together with the importance of accurate initial flow conditions and boundary conditions. A challenge for the numerical validation is to obtain suitable laboratory data sets of high quality with the relevant data typology. Another challenge is to validate simultaneously both the pressure and velocity fields. As one researcher explained, "*when the free-surface is right, the velocity field is typically wrong; if the velocity is right, the free-surface is usually wrong*" (P. Lubin 2008, Pers. Comm.).

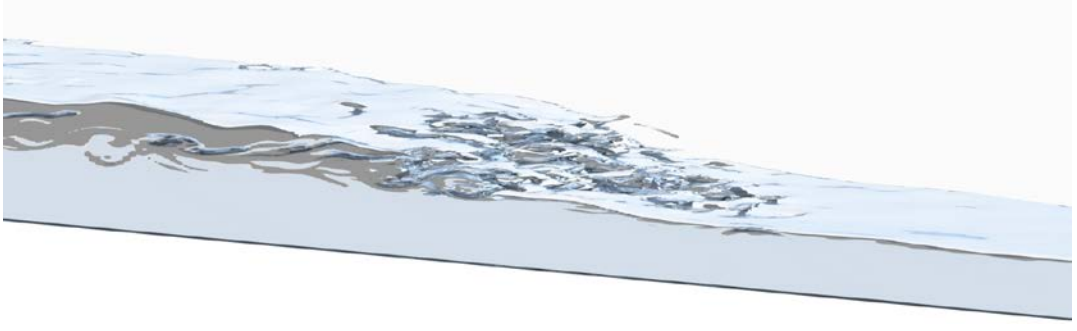

Figure 5 Tidal bore propagation in a rectangular channel (3D modelling) (Courtesy of Dr Pierre Lubin) - Flow conditions: Fr_1 = 1.77, d_1 = 0.0785 m, V_1 = 1.02 m/s, B = 0.5 m/s, t = 3.62 s after gate closure, bore propagation from left to right, laboratory data set: Koch and Chanson (2009), numerical data set: Chanson et al. (2012)

5 DISCUSSION

For more than twenty years, the author has been actively involved in tidal bore research. What are the key outcomes? It is thought that some basic outcomes encompassed a greater awareness of the physical process, together with a basic methodology for experimental measurements in laboratory and in the field, leading to a better understanding of the unsteady turbulent mixing, especially under controlled flow conditions. The last two decades saw a large number of general and scientific publications on tidal

bores, including a catalogue and a book (Bartsch-Winkler and Lynch 1988, Chanson 2011a) adding to existing documentations on the few notorious bores of the Qiantang, Seine and Severn rivers. Thrill-seeking activities and cultural events developed around some tidal bores during the last fifteen years in Asia, Europe and the Americas. In Europe and South America, tidal bore surfing competitions take place on the Dordogne River, Severn River, Araguari River and Rio Mearim. Some milestone laboratory experiments were performed by Hornung et al. (1995), Chanson (2005), Koch and Chanson (2008,2009) with a focus on turbulent mixing. These were complemented by some detailed field measurements (Table 1). On the other hand, the last two decades were marked possibly by too high expectations in terms of numerical modelling of tidal bores, including CFD, as well as some difficult field measurement conditions, illustrated by repeated incidents and loss of equipments. More our current knowledge into the transport of particulates by tidal bores remains minimal, but for a couple of studies (Tull 1997, Chanson and Tan 2010).

So what is the future of tidal bore research? In the author's opinion, the future research should rely upon (1) field measurements with fine temporal and spatial resolution, and (2) some composite modelling embedding physical and CFD numerical modelling. Despite the challenges, an important drive of future research must be some new field measurements, performed at full-scale in natural systems. Field works are essential because theoretical, numerical and physical models can only attempt to reproduce the prototype flow conditions within some crude assumptions. The extrapolation of model results might be subjected to some form of scale effects; simply no prototype data means no definite validation of any kind of modelling!

The hydraulics of tidal bores will greatly benefit from the insights provided by computational calculations combined with ad-hoc laboratory measurements. Physical and CFD modelling cannot be dissociated. New laboratory experiments must be developed to provide high-quality data sets with physical measurements relevant to the CFD validation. A proper validation of CFD modelling results should be at least based upon the time-variations of the distributions of pressure, mean velocity, turbulence intensity, turbulent integral length and time scales. A drawback of current CFD methods (DNS, LES) is the computational resources required to complete a simulation and the level of information necessary to describe the system boundary conditions, although future research directions must encompass sediment and particulate transport with innovative modelling techniques (e.g. Eulerian-Lagrangian modelling).

A major challenge with breaking tidal bores is the three-phase nature of the flow at the prototype scale: water, air bubbles and sediments, as illustrated in numerous photographs. In many breaking bores, a substantial entrainment of air bubbles takes place in the bore roller (Chanson 2009, Docherty and Chanson 2010), while the sediment load is large (Khezri and Chanson 2012) and the turbulent modulation in sediment-laden flows cannot be neglected (Jha and Bombardelli 2009). To date no study was undertaken in a three-phase flow with high sediment and air contents despite the physical relevance.

6 CONCLUSION

A tidal bore is a hydrodynamic shock propagating upstream as the tidal flow turns to rising. The tidal bore forms during spring tides when the tidal range exceeds 4.5-6 m and the flood tide is confined to a funnelled estuarine system with relatively low freshwater levels. The application of continuity and momentum principles gives a complete solution of the ratio of the conjugate cross-section areas as a function of the upstream Froude number $Fr_1 = (U+V_1)/(g \times A_1/B_1)^{1/2}$. The flow resistance is observed to decrease the ratio of conjugate depths for a given Froude number, while a downward bed slope tends to increase of the ratio d_2/d_1 for a fixed Froude number.

The tidal bore propagation induces a massive mixing of the natural system. Its occurrence is critical to the environmental balance of the estuarine zone. Prototype observations highlighted that the tidal bore passage is associated with large fluctuations in water depth and instantaneous velocity components. Both experimental and numerical studies indicated the production of large coherent structures advected behind the tidal bore. The existence of such energetic turbulent events beneath and shortly after the tidal bore front implied the generation of vorticity during the bore propagation, and indicated that a great amount of sediment materials could be placed into suspension and transported by the flood tide flow in a natural system. Importantly 'classical' mixing theories do not account for intense unsteady mixing generated by

the tidal bore motion.

Future research should combine computational calculations combined with ad-hoc laboratory measurements, and these must be complemented by detailed field measurements in natural systems. A key challenge is (and will be) the three-phase nature of the flow in natural systems, encompassing a highly turbulent flow, sediment scour and transport, and air bubble entrapment at the free-surface.

ACKNOWLEDGEMENTS

The author thanks all the people who provided him with valuable informations, including past and present students, co-workers, friends and relatives. He acknowledges the financial support of the University of Queensland, the Université de Bordeaux (I2M), the Australian Academy of Science and the Agence Nationale de la Recherche (Projet 10-BLAN-0911-01).

References

Bartsch-Winkler, S., and Lynch, D.K. 1988. Catalog of Worldwide Tidal Bore Occurrences and Characteristics. US Geological Survey Circular, No. 1022, 17 pages.

Bazin, H. 1865. Recherches Expérimentales sur la Propagation des Ondes. (Experimental Research on Wave Propagation.) Mémoires présentés par divers savants à l'Académie des Sciences, Paris, France, Vol. 19, pp. 495-644 (in French).

Benet, F., and Cunge, J.A. 1971. Analysis of Experiments on Secondary Undulations caused by Surge Waves in Trapezoidal Channels. Jl of Hydraulic Research, IAHR, Vol. 9, No. 1, pp. 11-33.

Chanson, H. 2005. Physical Modelling of the Flow Field in an Undular Tidal Bore. Journal of Hydraulic Research, IAHR, Vol. 43, No. 3, pp. 234-244.

Chanson, H. 2009. The Rumble Sound Generated by a Tidal Bore Event in the Baie du Mont Saint Michel. Journal of Acoustical Society of America, Vol. 125, No. 6, pp. 3561-3568 (DOI: 10.1121/1.3124781).

Chanson, H. 2010a. Undular Tidal Bores: Basic Theory and Free-surface Characteristics. Journal of Hydraulic Engineering, ASCE, Vol. 136, No. 11, pp. 940-944 (DOI: 10.1061/(ASCE)HY.1943-7900.0000264).

Chanson, H. 2010b. Unsteady Turbulence in Tidal Bores: Effects of Bed Roughness. Journal of Waterway, Port, Coastal, and Ocean Engineering, ASCE, Vol. 136, No. 5, pp. 247-256 (DOI: 10.1061/(ASCE)WW.1943-5460.0000048).

Chanson, H. 2011a. Tidal Bores, Aegir, Eagre, Mascaret, Pororoca: Theory and Observations. World Scientific Publ., Singapore, 220 pages.

Chanson, H. 2011b. Undular Tidal Bores: Effect of Channel Constriction and Bridge Piers. Environmental Fluid Mechanics, Vol. 11, No. 4, pp. 385-404 & 4 videos (DOI: 10.1007/s10652-010-9189-5).

Chanson, H. 2012. Momentum Considerations in Hydraulic Jumps and Bores. Journal of Irrigation and Drainage Engineering, ASCE, Vol. 138, No. 4, pp. 382-385 (DOI 10.1061/(ASCE)IR.1943-4774.0000409).

Chanson, H., Reungoat, D., Simon, B., and Lubin, P. 2011. High-Frequency Turbulence and Suspended Sediment Concentration Measurements in the Garonne River Tidal Bore. Estuarine Coastal and Shelf Science, Vol. 95, No. 2-3, pp. 298-306 (DOI 10.1016/j.ecss.2011.09.012).

Chanson, H., and Tan, K.K. 2010. Turbulent Mixing of Particles under Tidal Bores: an Experimental Analysis. Journal of Hydraulic Research, IAHR, Vol. 48, No. 5, pp. 641-649 (DOI: 10.1080/00221686.2010.512779).

Docherty, N.J., and Chanson, H. 2010. Characterisation of Unsteady Turbulence in Breaking Tidal Bores including the Effects of Bed Roughness. Hydraulic Model Report No. CH76/10, School of Civil Engineering, The University of Queensland, Brisbane, Australia, 112 pages.

Docherty, N.J., and Chanson, H. 2012. Physical Modelling of Unsteady Turbulence in Breaking Tidal Bores. Journal of Hydraulic Engineering, ASCE, Vol. 138, No. 5, pp. 412-419 (DOI: 10.1061/(ASCE)HY.1943-7900.0000542).

Furuyama, S., and Chanson, H. 2010. A Numerical Solution of a Tidal Bore Flow. Coastal Engineering Journal, Vol. 52, No. 3, pp. 215-234 (DOI: 10.1142/S057856341000218X).

Hornung, H.G., Willert, C., and Turner, S. 1995. The Flow Field Downsteam of a Hydraulic Jump. Jl of Fluid Mechanics, Vol. 287, pp. 299-316.

Jha, S.K., and Bombardelli, F.A. 2009. Two-phase modeling of turbulence in dilute sediment-laden, open channel flows. Environmental Fluid Mechanics, Vol. 9, pp. 237-266.

Khezri, N., and Chanson, H. 2012. Inception of Bed Load Motion beneath a Bore. Geomorphology, Vol. 153-154, pp. 39-47 & 2 video movies (DOI: 10.1016/j.geomorph.2012.02.006) (ISSN 0169-555X).

Kjerfve, B., and Ferreira, H.O. 1993. Tidal Bores: First Ever Measurements. Ciência e Cultura (Jl of the Brazilian Assoc. for the Advancement of Science), Vol. 45, No. 2, March/April, pp. 135-138.

Koch, C., and Chanson, H. 2008. Turbulent Mixing beneath an Undular Bore Front. Journal of Coastal Research, Vol. 24, No. 4, pp. 999-1007 (DOI: 10.2112/06-0688.1).

Koch, C., and Chanson, H. 2009. Turbulence Measurements in Positive Surges and Bores. Journal of Hydraulic Research, IAHR, Vol. 47, No. 1, pp. 29-40 (DOI: 10.3826/jhr.2009.2954).

Lemoine, R. 1948. Sur les Ondes Positives de Translation dans les Canaux et sur le Ressaut Ondulé de Faible Amplitude. (On the Positive Surges in Channels and on the Undular Jumps of Low Wave Height.) Jl La Houille

Blanche, Mar-Apr., pp. 183-185 (in French).
Liggett, J.A. 1994. Fluid Mechanics. McGraw-Hill, New York, USA.
Lighthill, J. 1978. Waves in Fluids. Cambridge University Press, Cambridge, UK, 504 pages.
Lubin, P., Chanson, H., and Glockner, S. 2010. Large Eddy Simulation of Turbulence Generated by a Weak Breaking Tidal Bore. Environmental Fluid Mechanics, Vol. 10, No. 5, pp. 587-602 (DOI: 10.1007/s10652-009-9165-0).
Madsen, P.A., Simonsen, H.J., and Pan, C.H. 2005. Numerical Simulation of Tidal Bores and Hydraulic Jumps. Coastal Eng., Vol. 52, pp. 409-433 (DOI: 10.1016/j.coastaleng.2004.12.007).
Moore, R.N. 1888. Report on the Bore of the Tsien-Tang Kiang. Hydrographic Office, London.
Mouazé, D., Chanson, H., and Simon, B. 2010. Field Measurements in the Tidal Bore of the Sélune River in the Bay of Mont Saint Michel (September 2010). Hydraulic Model Report No. CH81/10, School of Civil Engineering, The University of Queensland, Brisbane, Australia, 72 pages.
Moule, A.C. 1923. The Bore on the Ch'ien-T'ang River in China. T'oung Pao, Archives pour servir à l'étude de l'histoire, des langues, la geographie et l'ethnographie de l'Asie Orientale (Chine, Japon, Corée, Indo-Chine, Asie Centrale et Malaisie), Vol. 22, pp. 10-188.
Reichstetter, R. 2011. Hydraulic Modelling of Unsteady Open Channel Flow: Physical and Analytical Validation of Numerical Models of Positive and Negative Surges. MPhil thesis, School of Civil Engineering, The University of Queensland, Brisbane, Australia, 112 pages.
Reungoat, D., Chanson, H., and Caplain, B. 2012. Field Measurements in the Tidal Bore of the Garonne River at Arcins (June 2012). Hydraulic Model Report No. CH89/12, School of Civil Engineering, The University of Queensland, Brisbane, Australia, 121 pages.
Simon, B., Lubin, P., Glockner, S., and Chanson, H. 2011. Three-Dimensional Numerical Simulation of the Hydrodynamics generated by a Weak Breaking Tidal Bore. Proceedings of 34th IAHR World Congress, Brisbane, Australia, 26 June-1 July, Engineers Australia Publication, Eric Valentine, Colin Apelt, James Ball, Hubert Chanson, Ron Cox, Rob Ettema, George Kuczera, Martin Lambert, Bruce Melville and Jane Sargison Editors, pp. 1133-1140.
Simpson, J.H., Fisher, N.R., and Wiles, P. 2004. Reynolds Stress and TKE Production in an Estuary with a Tidal Bore. Estuarine, Coastal and Shelf Science, Vol. 60, No. 4, pp. 619-627.
Tanaka, N., Yagisawa, J., and Yasuda, S. 2012. Characteristics of Damage due to Tsunami Propagation in River Channels and Overflow of their Embankments in Great East Japan Earthquake. International Journal of River Basin Management, Vol. 10, No. 3, pp. 269-279.
Tricker, R.A.R. 1965. Bores, Breakers, Waves and Wakes. American Elsevier Publ. Co., New York, USA.
Tull, K.A. 1997. Spawning Activity of triped Bass in a Tidal Bore River: the Shubenacadie-Stewiacke System, Nova Scotia. M.Sc. thesis, University of East Carolina, Dept of Biology, 140 pages.
Wolanski, E., Williams, D., Spagnol, S., and Chanson, H. (2004). "Undular Tidal Bore Dynamics in the Daly Estuary, Northern Australia." Estuarine, Coastal and Shelf Science, Vol. 60, No. 4, pp. 629-636 (DOI: 10.1016/j.ecss.2004.03.001).